Applied Catalysis B: Environment and Energy 348 (2024) 123835

Contents lists available at ScienceDirect

Applied Catalysis B: Environment and Energy

journal homepage: www.elsevier.com/locate/apcatb

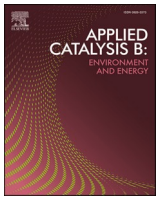

Thioxanthone-based ionic liquid as photocatalyst for a tandem cyclization reaction to synthesize pyrroloquinolinones

Huixin Tong, Mengqi Zou, Yuli Sha, Weiya Zhang, Houhai Fan, Zhizhong Sun, Wenyi Chu *

School of Chemistry and Materials Science, Heilongjiang University, Harbin 150080, PR China

ARTICLE INFO

Keywords:
Tandem cyclization
Pyrroloquinolinone
Bifunctional catalyst
Thioxanthone
Ionic liquids

ABSTRACT

Visible light catalysis provides an important platform for developing green and sustainable catalytic processes. However, traditional photosensitizers have limited their application due to their inherent limitations. Due to the structural stability and recyclability of ionic liquids (ILs), a bifunctional catalyst **TXIL-Ni** was designed and synthesized by introducing the photosensitizer thioxanthone (TX) and transition metal **Ni(II)** into ILs. **TXIL-Ni** exhibited remarkable photocatalytic activity for C7–H acylation of indolines to efficiently synthesize pyrroloquinolinone derivatives by a tandem cyclization reaction of decarboxylation acylation and Claisen-Schmidt condensation. The protocol provided a new strategy for the synthesis of the natural product Viridicatol and the key intermediate of farnesyltransferase inhibitors. The experimental results indicated that thioxanthone-based ionic liquid **TXIL-Ni** as a synergistic photocatalyst has the advantages of mild reaction conditions, recyclability, and atomic economy. This provides a new solution for the design of multifunctional and reusable catalysts.

1. Introduction

Pyrroloquinolinones, as an important N-heterocyclic skeleton, are often found as a core structure in pesticides, natural products, bioactive molecules, and optoelectronic materials [1,2]. Due to their extensive biological and pharmacological activities, they are applied in drug molecules, such as antiasthma drugs [3], antiepileptic drugs [4], anticonvulsant drugs [5], and anti-cancer drugs [6]. For example, pyrroloquinolinone, as a core structure, is found in the natural alkaloid Oxoassoanine [7] and applied to the optoelectronic material HPPCO and DCQTB [8], and pyrroloquinolinone derivatives also are used as important intermediate in the synthesis of efficient and highly selective anticancer drug farnesyltransferase inhibitors (FTIs) [9–12] as shown in Fig. 1.

It is precisely because pyrroloquinolinone derivatives play important roles in natural products and pharmaceutical chemistry that their synthesis has attracted widespread attention. The conventional synthesis methodologies mostly depend on thermos-catalytic cyclization reactions to construct pyrroloquinolinone skeletons [13–17], such as Fischer indole cyclization and Michael-type cyclization, and so on. These conversion methods are effective, but they have some drawbacks such as the use of toxic solvents and cumbersome procedures. Subsequently, inspired by C–H activation [18], the research groups of Loh, Jeganmohan, and Sundararaju reported the use of indoline derivatives as starting materials through transition-metal catalyzed C–H functionalization and cyclization reaction to effectively construct pyrroloquinolinone derivatives (Scheme 1a) [19–23]. Although these strategies are effective, expensive metal catalysts, high reaction temperatures, stoichiometric redox reagents, and difficulty in recovering catalysts greatly hinder their widespread application. In recent years, visible light as a green and sustainable energy source has been widely utilized to activate organic chemical conversion [24,25]. Compared with the conventional strategy, photocatalytic reactions have clear advantages: friendly to the environment, mild reaction conditions, and high atom utilization. The construction of complex molecules through visible light-induced C–H functionalization has become a hot subject, and many thermocatalytic reactions can be readily achieved by using photoexcitation, especially visible light-induced decarboxylation coupling [26–29]. At present, although some photocatalytic C–H activation reactions have achieved, there are still some limitations in these methods. The main photosensitizers for visible light-catalyzed organic conversion are Ru (II) and Ir (III), which are rare and expensive elements [30]. Organic dyes, as potential substitutes, also have the disadvantage of difficult recovery [31–35]. Therefore, the development of environmentally friendly and

* Corresponding author.
E-mail address: wenyichu@hlju.edu.cn (W. Chu).

https://doi.org/10.1016/j.apcatb.2024.123835
Received 18 December 2023; Received in revised form 7 February 2024; Accepted 9 February 2024
Available online 13 February 2024

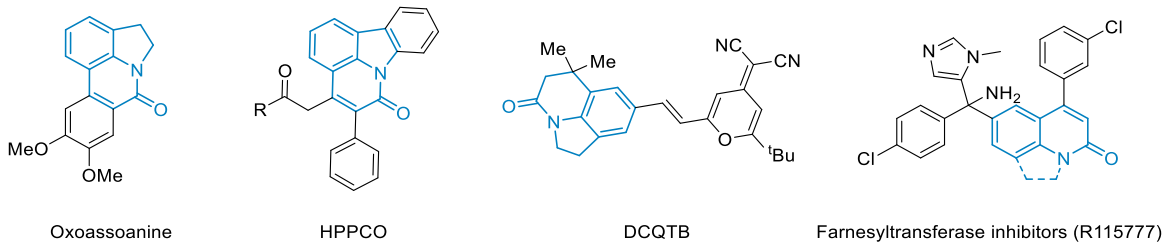

Fig. 1. Some representative molecules containing pyrroloquinolinone core.

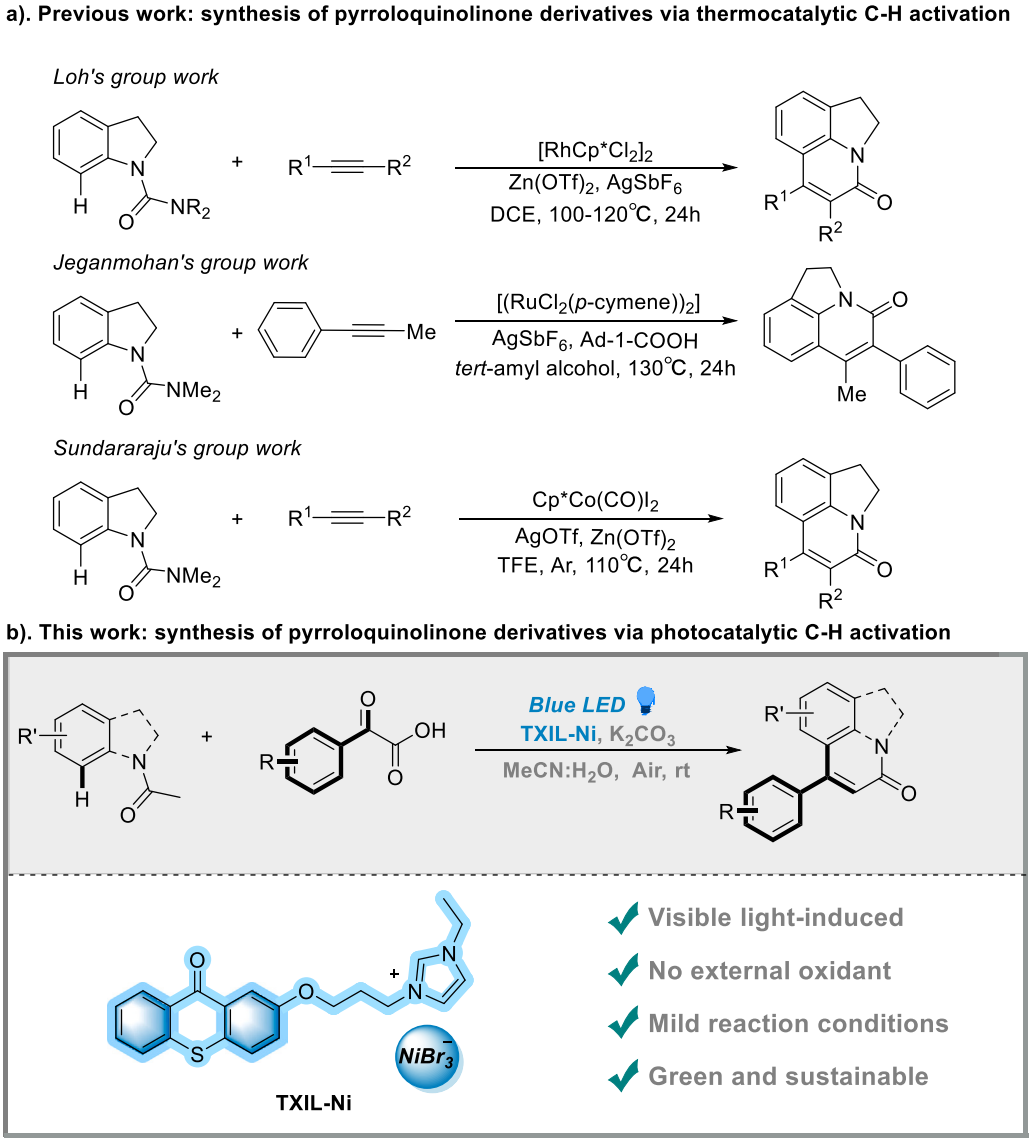

Scheme 1. Reported works and our work for synthesis of pyrroloquinolinone derivatives.

sustainable methods for the synthesis of pyrroloquinolinones has become a focus of current research.

Ionic liquids (ILs), as a substitute for green design, provide a powerful multifunctional platform for designing new multifunctional catalysts and sustainable strategies [36–38]. ILs can act as the solvent, ligand, and support as well as bio-, photo- and electro-catalysts, potentially achieving more green and sustainable processes [39–43]. It is possible to design specific functionalized ILs with desirable properties for specific chemical reactions by combining a variety of cations and anions with characteristic structures [44–47]. For traditional homogeneous catalysts, they have low sustainability and high environmental impact. However, due to their high sustainability and designability, ILs can be adjusted to a certain extent according to different reaction requirements to design green catalysts with synergistic catalytic capabilities. Hence, based on the designability of ILs, it is of great significance to design and synthesize a task-specific ionic liquid photocatalyst for visible-light-induced C–H functionalization /intramolecular cyclization reaction to synthesize the pyrroloquinolinones in one-pot.

Herein, we report that a novel ionic liquid photocatalyst **TXIL-Ni** containing thioxanthone photosensitizer and transition metals was

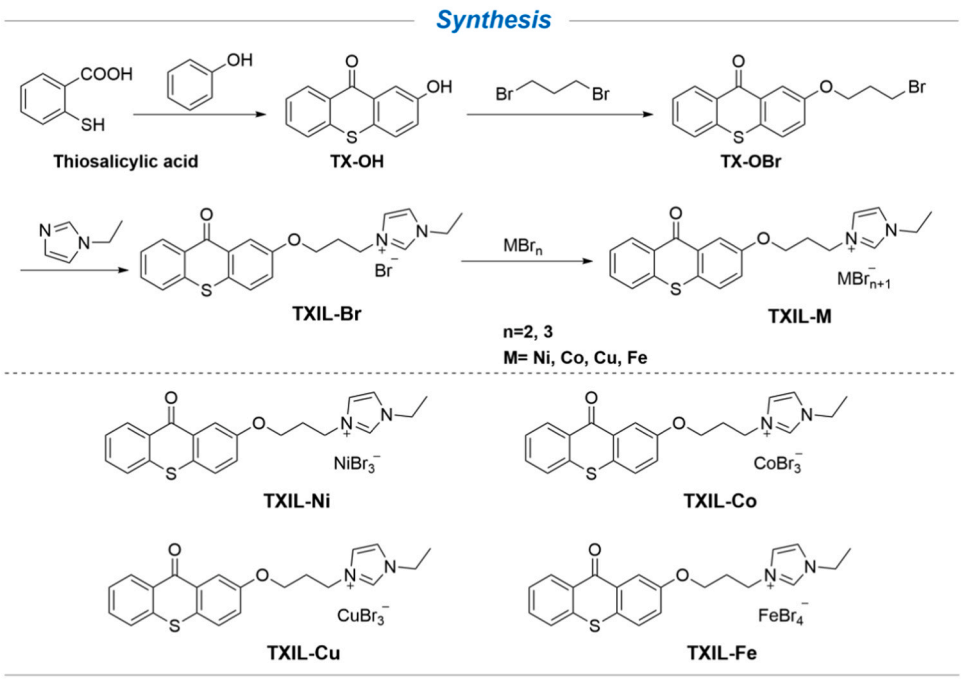

Scheme 2. The synthetic route of **TXIL-M.**

prepared by introducing the organic dye thioxanthone (TX) into the imidazole based ionic liquid and conducting anion exchange with metal halides. Compared with TX, **TXIL-Ni** was more easily excited by blue LED light, and the introduction of metal anions effectively realized the role of metal catalysis. **TXIL-Ni** was applied as an organic photocatalyst for a tandem cyclization reaction of decarboxylation acylation and Claisen-Schmidt reaction to prepare pyrroloquinolinones (Scheme 1b). Various optical performance tests demonstrated that **TXIL-Ni** exhibited superior photophysical, low excitation energy, and well cycling property than organic dye TX, which was ascribed to their excellent light capture ability and various catalytic functions. Compared with traditional photosensitizers and expensive transition metal catalysts, **TXIL-Ni** overcame the limitations of using organic photocatalysts and solid metal salts alone, providing an environmentally friendly new method for the construction of pyrroloquinolinones.

2. Experimental section

2.1. Materials

All materials and the reagents used in this work were bought from commercial suppliers and used without further purification.

2.2. Synthesis of ionic liquid photocatalysts

The synthesis method of bifunctional ionic liquids photocatalysts was shown in Scheme 2. Thiosalicylic acid was used as the starting material by a cyclization reaction with phenol to obtain 2-hydroxybenzophenone. Next, 2-hydroxythioxanthone underwent the etherification reaction with 1,3-dibromopropane, followed by covalently linking to 1-ethylimidazole to form imidazole cation, and finally obtaining thioxanthone-based ionic liquid photosensitizers through anion exchange with different metal halides. Specific synthesis steps and the spectroscopic characterizations were included in the supporting information (**SI**).

2.3. Catalyst characterization

All the characterizations of the structure and photophysical properties of the thioxanthone-based ionic liquid photocatalyst were implemented via various techniques. The specific information on testing conditions, DFT calculations, and quantum yield calculations were presented in the **SI** for details.

3. Results and discussion

3.1. Analysis of photocatalytic ability of TXIL-M

To understand the photocatalytic capacity of **TXIL-M**, visible-light-induced indolines C7–H acylation/intramolecular cyclization reaction were performed for the synthesis of pyrroloquinolinones using *N*-acetylindoline (**1a**) and α-oxophenylacetic acid (**2a**) as the template substrates, and the experimental results were depicted in Table 1. Firstly, four ionic liquid photocatalysts were used as the catalysts for the tandem cyclization reaction in acetonitrile (MeCN)/H_2O (V: V=2: 1) in the presence of K_2CO_3 under the irradiation of a blue LED at room temperature for 24 h. To our delight, the desired product (**3a**) was obtained with a yield of 60% by using **TXIL-Co** as the photocatalyst (Table 1, **entry 1**). **TXIL-Cu** and **TXIL-Fe** as the photocatalysts only afforded **3a** in the yields of 43% and 31%, respectively (Table 1, **entries 2** and **3**), while **TXIL-Ni** as the photocatalyst provided the product **3a** with the yield of up to 86% (Table 1, **entry 4**). Furthermore, other transition metal catalysts and organic photocatalysts were screened, and thioxanthone (**I**), Mes-Acr-$MeClO_4$ (**II**), $[Ir(ppy)_2(dtbbpy)]PF_6$ (**III**) and $Ru(bpy)_3(PF_6)_2$ (**IV**) were employed to obtain the target product **3a** with the yields of 0%, 0%, 59%, and 46%, respectively (Table 1, **entries 5–8**). Next, the reaction medium was screened as an important factor affecting the reaction conversion. *N,N*-dimethylformamide (DMF)/H_2O (V: V=2: 1) was used as reaction solvent, and the yield of the product **3a** only was 58% (Table 1, **entry 9**). Methanol (MeOH)/H_2O (V: V=2: 1) and ethyl alcohol (EtOH)/H_2O (V: V=2: 1) as the solvents obtained the product **3a** with a lower yield of 21% and 17%, respectively (Table 1, **entries 10** and **11**). Tetrahydrofuran (THF)/H_2O (V: V=2: 1) as the solvent gave the product in the yield of 42% (Table 1, **entry 12**). The yield of **3a** provided

Table 1
Optimization of reaction conditions.[a].

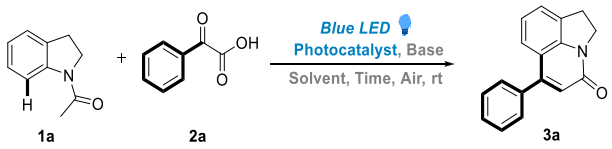

entry	catalyst (mol%)	solvent (V: V)	base (equiv.)	yield (%)[b]
1	**TXIL-Co** (10)	MeCN: H_2O (2:1)	K_2CO_3	60
2	**TXIL-Cu** (10)	MeCN: H_2O (2:1)	K_2CO_3	43
3	**TXIL-Fe** (10)	MeCN: H_2O (2:1)	K_2CO_3	31
4	**TXIL-Ni** (10)	MeCN: H_2O (2:1)	K_2CO_3	86, 63[c], 85[d]
5	**I** (10)	MeCN: H_2O (2:1)	K_2CO_3	0
6	**II** (10)	MeCN: H_2O (2:1)	K_2CO_3	0
7	**III** (10)	MeCN: H_2O (2:1)	K_2CO_3	59
8	**IV** (10)	MeCN: H_2O (2:1)	K_2CO_3	46
9	**TXIL-Ni** (10)	DMF: H_2O (2:1)	K_2CO_3	58
10	**TXIL-Ni** (10)	MeOH: H_2O (2:1)	K_2CO_3	21
11	**TXIL-Ni** (10)	EtOH: H_2O (2:1)	K_2CO_3	17
12	**TXIL-Ni** (10)	THF: H_2O (2:1)	K_2CO_3	42
13	**TXIL-Ni** (10)	MeCN	K_2CO_3	60
14	**TXIL-Ni** (10)	MeCN: H_2O (1:1)	K_2CO_3	69
15	**TXIL-Ni** (10)	MeCN: H_2O (1:2)	K_2CO_3	63
16	**TXIL-Ni** (10)	MeCN: H_2O (2:1)	$NaHCO_3$	70
17	**TXIL-Ni** (10)	MeCN: H_2O (2:1)	Na_2CO_3	77
18	**TXIL-Ni** (10)	MeCN: H_2O (2:1)	NaOH	61
19	**TXIL-Ni** (10)	MeCN: H_2O (2:1)	Et_3N	39
20	**TXIL-Ni** (10)	MeCN: H_2O (2:1)	DBU	44
21	**TXIL-Ni** (5)	MeCN: H_2O (2:1)	K_2CO_3	71
22	**TXIL-Ni** (15)	MeCN: H_2O (2:1)	K_2CO_3	87
23	–	MeCN: H_2O (2:1)	K_2CO_3	0

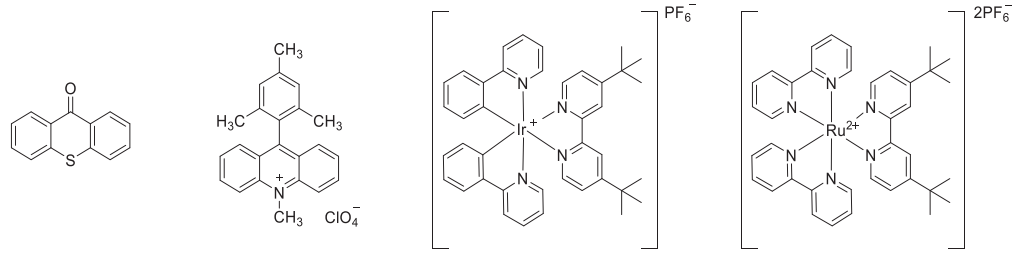

Thioxanthen-9-one (TX) I | Mes-Acr-$MeClO_4$ II | $[Ir(ppy)_2(dtbbpy)]PF_6$ III | $Ru(bpy)_3(PF6)_2$ IV

[a]Reaction conditions: **1a** (0.3 mmol), **2a** (0.45 mmol), photocatalyst (10 mol%) and base (4 equiv.) in solvent (3.0 mL) under blue LED irradiation at room temperature for 24 h (monitored by TLC).[b]Isolated yields.[c,d]Reaction time: 12 h and 48 h, respectively.

60% when MeCN was selected as reaction solvent (Table 1, **entry 13**). Subsequently, the yield of the product **3a** reduced after increasing the proportion of water in the mixed solvent, which may be caused by a decrease in the solubility of the substrate (Table 1, **entries 14** and **15**). The result showed that MeCN/H_2O (V: V=2: 1) was the appropriate choice as the reaction solvent. Then, the effects of different bases on the reaction were investigated including organic and inorganic bases. For inorganic bases, $NaHCO_3$ and Na_2CO_3 were used as the bases to give the product with yields of 70% and 77%, respectively (Table 1, **entries 16** and **17**), and NaOH only gave the product with yield of 61% (Table 1, **entry 18**). For organic bases, triethylamine (Et_3N) and 1,8-diazabicyclo-bicyclo-(5,4,0)–7-undecane (DBU) were used as the bases to only give the product with the yields of 39% and 44%, respectively (Table 1, **entries 19** and **20**). Finally, the effect of the amount of photocatalysts and reaction time on the reaction was investigated. It was found that the yield of the product did not significantly change with the increase of the amount of the photocatalyst **TXIL-Ni** (Table 1, **entries 21** and **22**) and the prolongation of reaction time (Table 1, **entries 4[c]** and **4[d]**). In addition, no target product was obtained without adding **TXIL-Ni** (Table 1, **entry 23**).

Therefore, according to the above experiments, the optimized reaction conditions were chosen: 10 mol% of **TXIL-Ni** as the photocatalyst and K_2CO_3 as the base in MeCN/H_2O (V: V=2: 1) under blue light irradiation at room temperature for 24 h under an air atmosphere.

3.2. *The structure and photophysical properties of TXIL-Ni*

The structure of **TXIL-Ni** was further confirmed through X-ray diffraction (XRD) analysis and Fourier transform infrared (FT-IR) spectra. It was observed that the yellow solid powder **TXIL-Br** turned green after anion exchanged with $NiBr_2$ as shown in Fig. 2a, indicating the formation of a new species **TXIL-Ni**. Moreover, its structure was analyzed by XRD diffraction as shown in Fig. 2b, and it was found that in the wide-angle XRD spectrum of **TXIL-Ni**, the weak diffraction peaks at 14.48 °, 28.08 °, and 33.96 ° correspond to the (003), (101), and (104) lattice planes of $NiBr_2$ (PDF # 24–0789), respectively. In addition, FT-IR spectra were utilized to further determine the structure and functional groups of **TXIL-Ni** as shown in Fig. 2c. The above results indicated that

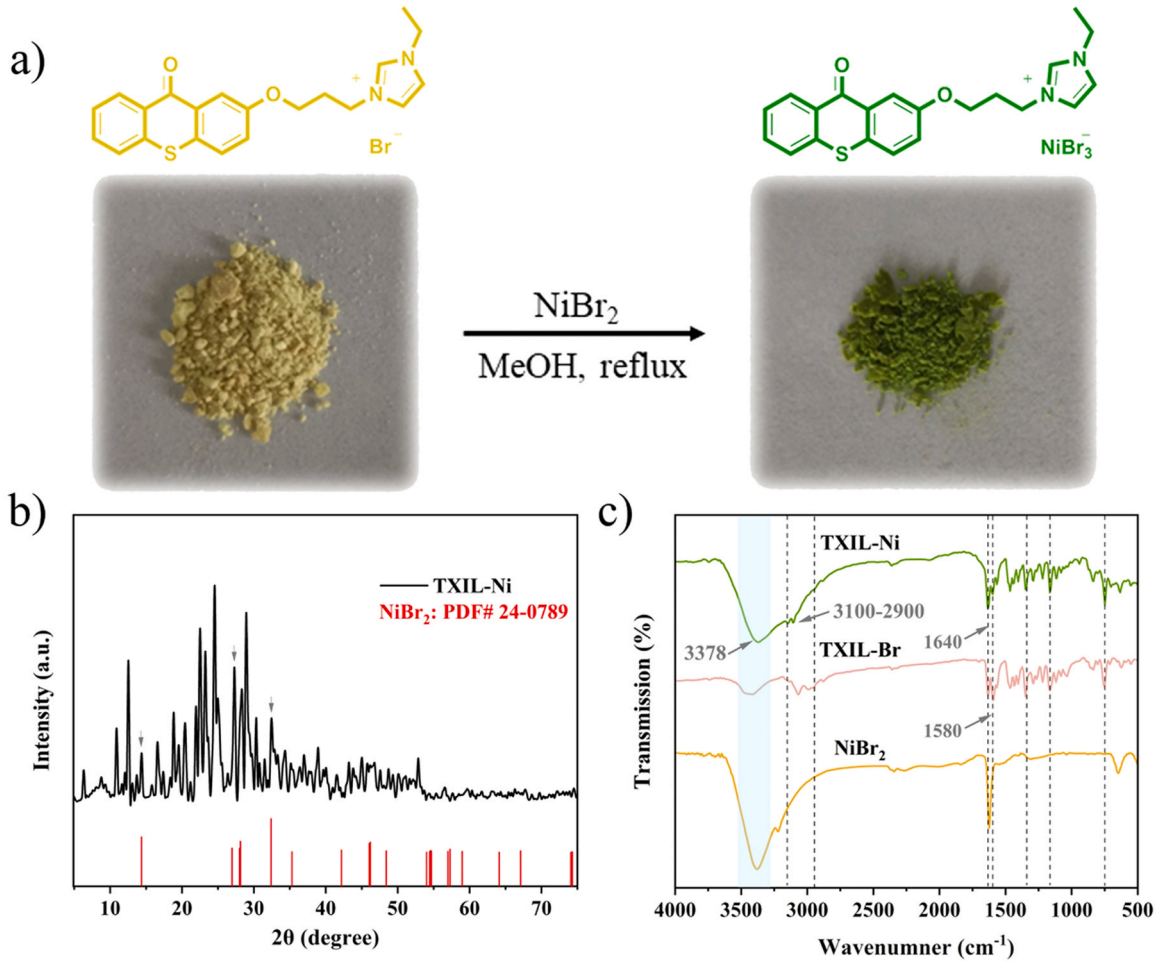

Fig. 2. (a) The structure and state of **TXIL-Ni**; (b) XRD patterns of **TXIL-Ni** and (c) FTIR spectra of **TXIL-Ni, TXIL-Br** and **$NiBr_2$**.

the thioxanthone-based ionic liquid **TXIL-Ni** was successfully prepared.

Next, a variety of measurements were conducted to gain properties of potential optical and electronic properties of **TXIL-Ni**. The UV–Vis absorption of the four synthesized ionic liquid photosensitizers and TX was represented as a composite spectrum for comparison as shown in Fig. 3a. Although four photocatalysts display similar absorption wavelengths, **TXIL-Ni** exhibited a higher absorbance compared to the parent thioxanthone core and several other catalysts. Compared with TX, the maximum absorption wavelength of **TXIL-Ni** was 397 nm and caused a bathochromic shift, accordingly, blue LED was chosen as the irradiation light source. In the fluorescent spectra, red-shifted peaks were observed for **TXIL-Ni** compared to TX as shown in Fig. 3b, and the photophysical properties of **TXIL-Ni** showed that its singlet lifetime was significantly extended ($\tau_s = 5.08$ ns) as shown in Fig. 3c. Furthermore, computational studies using (time-dependent) density functional theory indicated that **TXIL-Ni** ($E_{ex} = 3.23$ eV) had a lower photocatalyst excitation energy than TX ($E_{ex} = 3.60$ eV), so it was easier to be excited by visible light as shown in Fig. 3d. According to the cyclic voltammetry measurement, the half-wave potentials were determined as –0.41 V *vs* SCE, which can be assigned to the **TXIL-Ni**/**TXIL-Ni**$^{\bullet-}$ couple. Upon irradiation with visible light, **TXIL-Ni** can undergo photoexcitation to give excited species **TXIL-Ni***. Compared with TX* ($E_{p/2}$ (TX*/TX$^{\bullet-}$) = +1.67 V *vs* SCE), the **TXIL-Ni*** had a dramatically enhanced oxidative capability ($E_{p/2}$ (**TXIL-Ni***/**TXIL-Ni**$^{\bullet-}$) = +2.50 V *vs* SCE) as shown in Fig. 3e. Ultimately, electrochemical impedance test (EIS) analysis showed that under the same conditions, the semicircle diameter of the Nyquist diagram of **TXIL-Ni** was smaller, and the resistance to electron transfer and chemical reaction was smaller as shown in Fig. 3f. Consequently, effective electron transfer or charge transfer can occur under light excitation. The above experimental results indicated that **TXIL-Ni** exhibits excellent photochemical properties, which also confirmed that it can be used as a novel photocatalyst with a relatively easy photoexcitation nature.

3.3. Substrate scopes

Under the optimized reaction conditions, the substrate scope and limitations of this reaction were investigated as shown in Scheme 3. Firstly, the effect of the substituent groups of α-oxophenylacetic acids on the product yield was investigated. The reactions preceded smoothly using α-oxophenylacetic acids with both electron-rich and electron-deficient groups as the substrates. According to the experimental results, α-oxophenylacetic acid could obtain the target product **3a** in 86% yield. For the substituents at *para*-position, the electron-donating groups −Me and −OMe gave the corresponding products **3b** and **3c** with excellent yields of 87% and 90%. Compared to the electron-donating groups, the electron-withdrawing groups −Br, −Cl, −F gave the product **3d**-**3 f** with slightly low yields of 78%, 76%, and 69%, respectively. For the substituents at *meta*- position, the electron-donating group −Me obtained the target product **3 g** in 85% yield, and the electron-withdrawing groups −Br, −Cl, and −F afforded the products **3 h**, **3i**, and **3j** with the yields of 76%, 75%, and 67%, respectively. For the substituents at *ortho*- position, the electron-donating group −Me obtained the target product **3k** in 81% yield, and the electron-withdrawing groups −Br, −Cl and −F afforded the products **3 l**, **3 m**, and **3 n** with slightly low yields of 74%, 71%, and 66%, respectively. Compared with *para*- and *meta*- substituents, *ortho*-

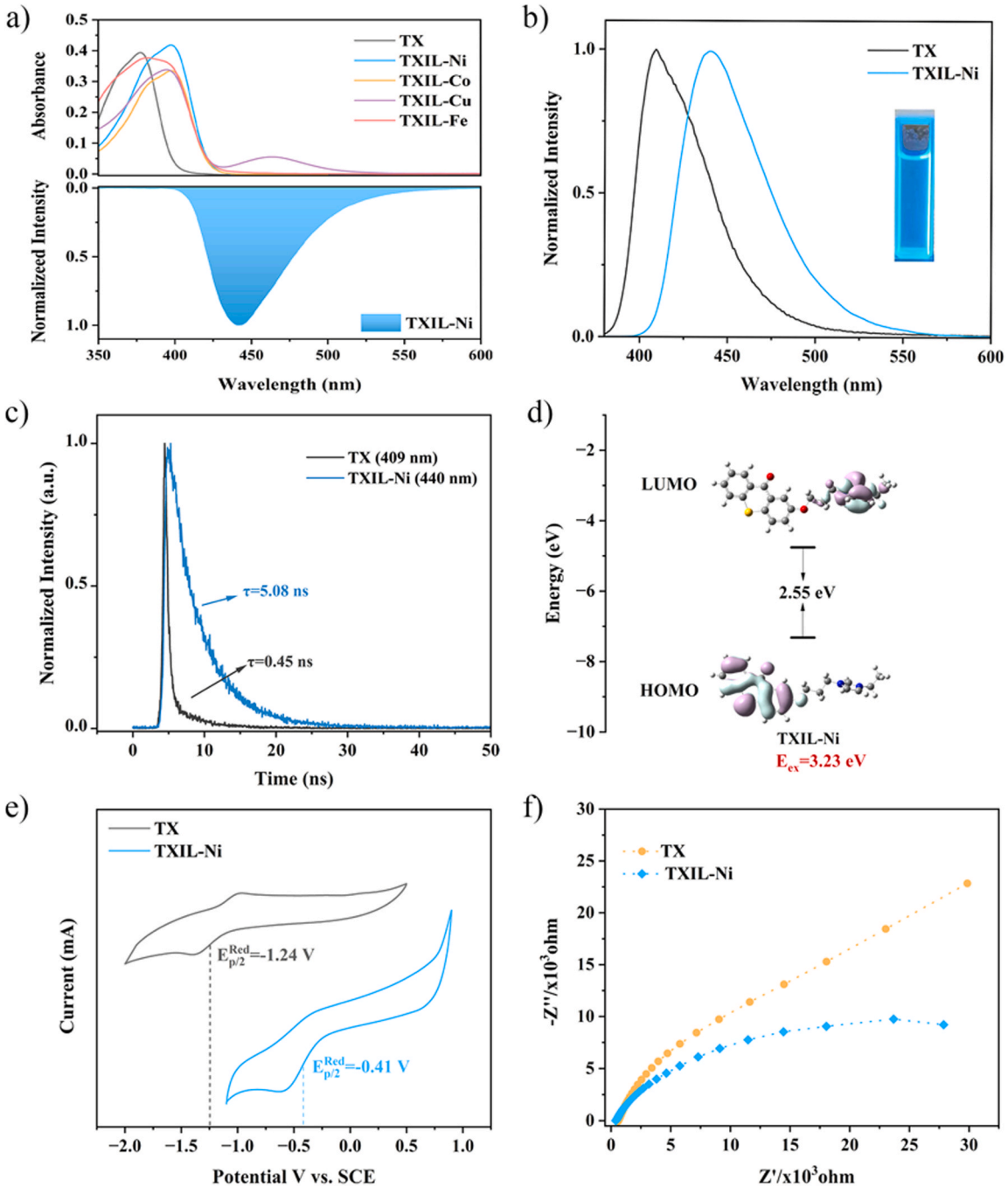

Fig. 3. The properties of the photocatalyst **TXIL-Ni:** (a) Absorbance profiles for **TX**, **TXIL-Ni**, **TXIL-Co**, **TXIL-Cu**, and **TXIL-Fe** in MeCN (0.1 mM); (b) Fluorescence emission spectra (Ex (TX) = 388 nm, Ex (**TXIL-Ni**) = 397 nm) in MeCN (0.1 mM); (c) Fluorescence lifetime profiles for TX and **TXIL-Ni** in MeCN (0.1 mM); (d) Excited-state energies calculated using the TD-DFT method for **TXIL-Ni** (for details to see the **SI**); (e) Cyclic voltammetry of **TX** and **TXIL-Ni** (for details to see the **SI**); (f) EIS Nyquist plots of **TX** and **TXIL-Ni**.

substituents caused a decrease in the yields of the products due to steric-hindrance effects. The above experimental results showed that the electron-donating groups are more favorable to the reaction than the electron-withdrawing groups. In addition, for multiple substitutions, corresponding products could also be obtained with good yields (**3o**, 87%).

Furthermore, a wide range of *N*-acetylindoline derivatives with different electronic properties and substitution patterns was investigated. Among them, the substituent −Me and −Ph at the C2 position of the indoline ring gave the product **3p** and **3q** with yields of 80% and 78%, while the substituent −Me at the C3 position of the indoline ring gave the product **3r** with the excellent yield of 82%. For the substituents at the C4 position of the indoline ring, the electron-donating −Me afforded the corresponding product **3 s** with the yield of 76%, while the electron-withdrawing groups –Cl and −F afforded the products **3 t** and **3 u** with good yields of 79% and 83%, respectively. For the substrates with the substituents (−CH_3, −OCH_3, and −Br) at the C5 position of the indoline ring gave the corresponding products in satisfactory yields (**3 v**, 80%; **3w**, 77%; **3x**, 81%). For the substituents at the C6 position of the indoline ring, the electron-donating group −CH_3 only afforded the product **3 y** in 60% yield. In addition, disubstituted product **3z** was also given smoothly in 70% yield. According to the above experimental

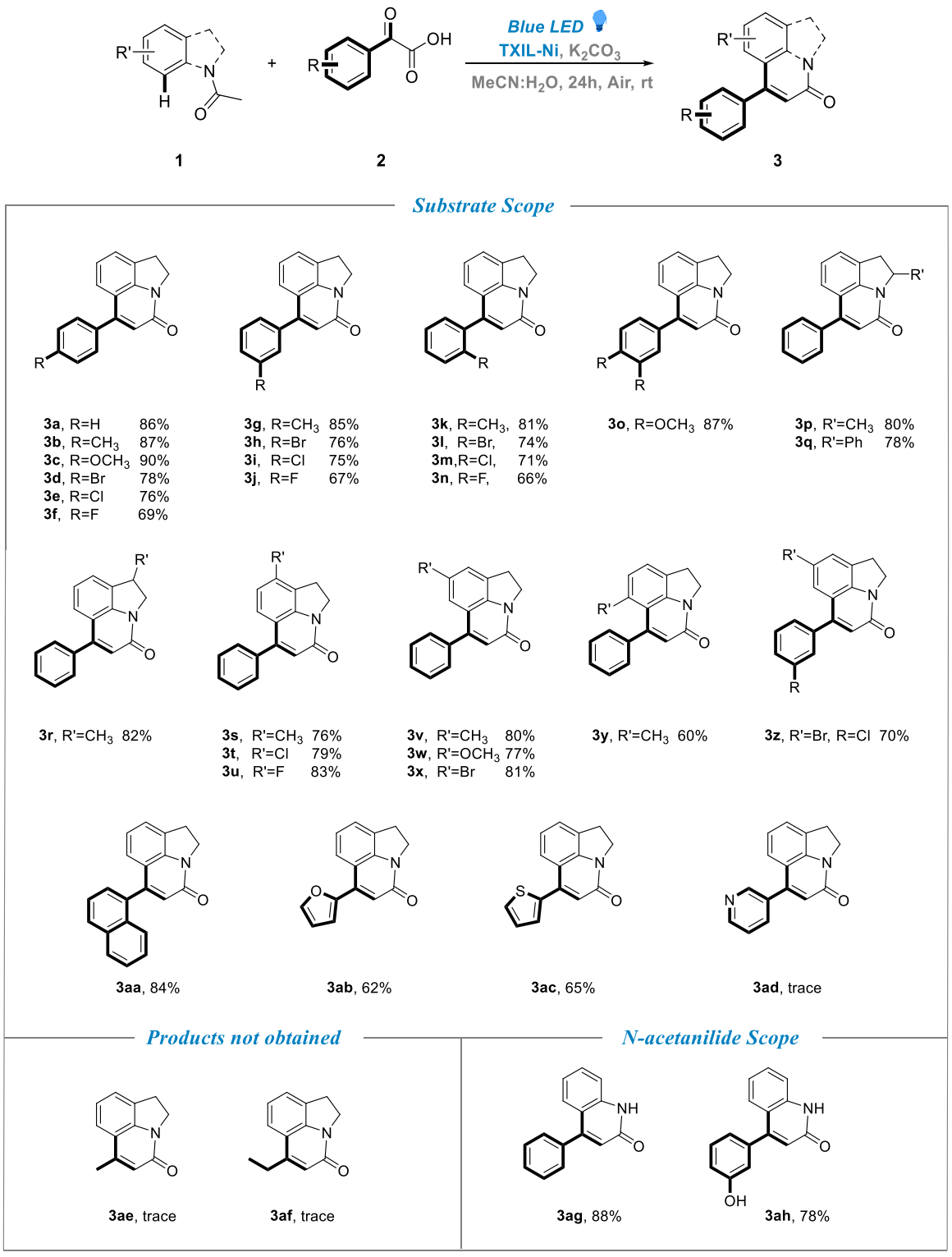

Scheme 3. Substrates scope of pyrroloquinolinone.[a b.] [a]*Reaction conditions:* **1** (0.3 mmol), **2** (0.45 mmol) and K_2CO_3 (4 equiv.), **TXIL-Ni** (10 mol%) in of MeCN: H_2O=2:1 (3.0 mL) under the irradiation of blue LED at room temperature for 24 h. [b]*Isolated yield by flash column chromatography.*

results, for the indoline moiety, the electron-withdrawing groups are more favorable to the reaction than the electron-donating groups, and the steric hindrance effect of the substituents at the C6 position is more pronounced than at other positions.

Moreover, other α-oxoacetic acids were also evaluated, and it was found that α-oxo-1-naphthylacetic acid obtained the corresponding product **3aa** with a good yield of 84%, and α-oxo-2-furanacetic acid, and α-oxo-2-thiopheneacetic acid obtained the corresponding products **3ab** and **3ac** in 62% and 65% yields. Unfortunately, α-oxo-3-pyridineacetic acid, α-oxopropanoic acid and α-oxobutyric acid did not obtain the corresponding product. It was noteworthy that acetanilide was also suitable for this system, and the corresponding products **3ag** and **3ah** were given with yields of 88% and 68%, among them, **3ah** is the precursor of the natural product Viridicatol [48].

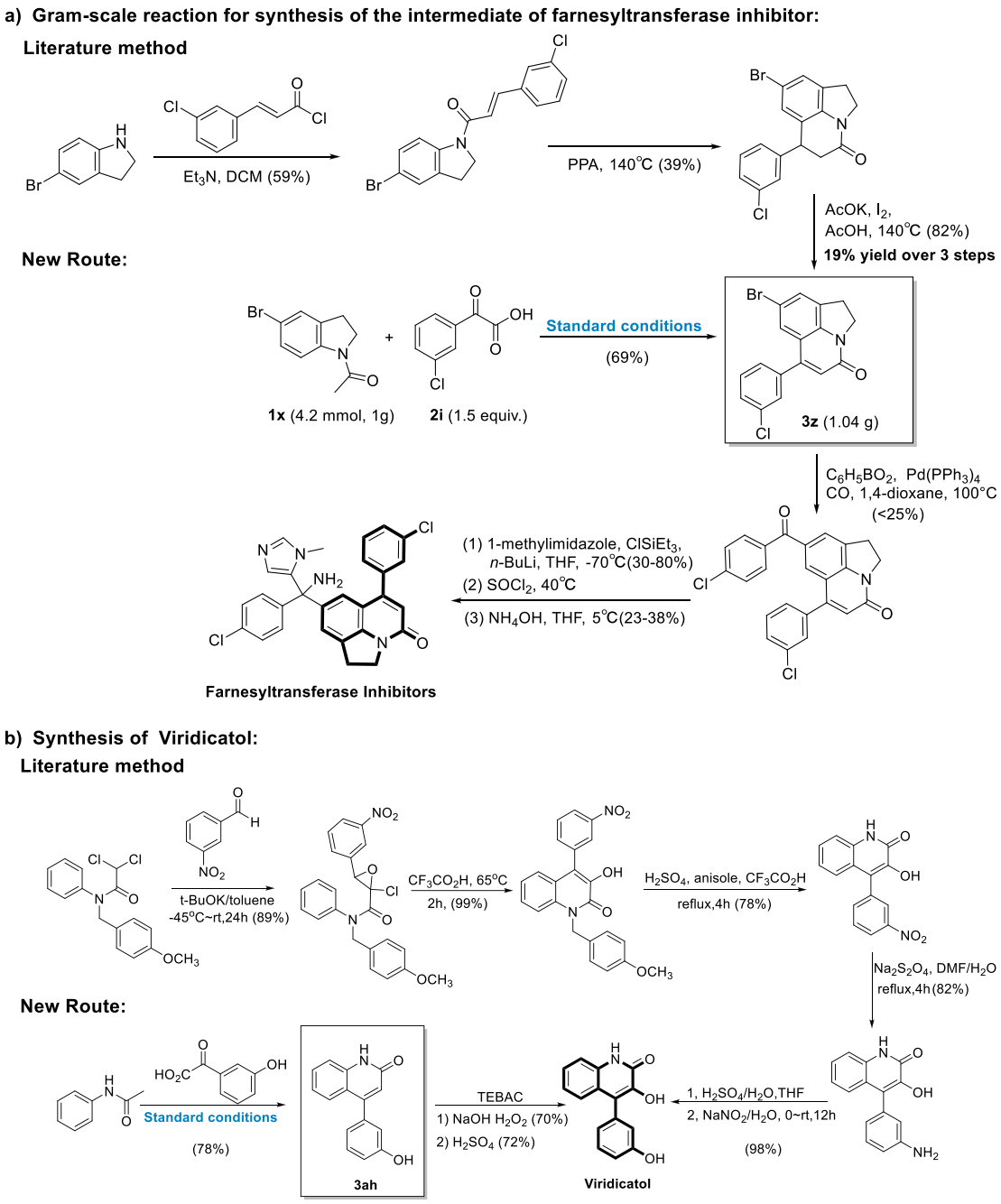

Scheme 4. (a) Gram-scale reaction for synthesis of the intermediate of farnesyltransferase inhibitor; (b) Synthesis of Viridicatol.

In order to further prove the effectiveness of this protocol, we conducted a gram scale experiment of the product **3z** (Scheme 4a). The reaction efficiency was still good after the reaction scale was increased, and the target product **3z** was obtained with the yield of 69%. The obtained product **3z** could be used as an intermediate to prepare the farnesyltransferase inhibitors [49–51], which is a class of molecularly targeted anti-tumor drugs under trial. Compared with the literature scheme, the new strategy has the advantages of mild reaction conditions, simple operation, and high yield.

In addition, this protocol could also be utilized for the synthesis of a natural product Viridicatol, which is a quinolone alkaloid with strong antifungal activity (Scheme 4b). Compared with the literature method [52], new protocol has the advantages of a simple reaction route, atom economy, and sustainability.

3.4. Reaction mechanism

In order to better explore the reaction mechanism, a series of control experiments were conducted as shown in Scheme 5. Under standard conditions, the radical inhibition experiment was conducted by the addition 1,1-diphenylethylene (2.0 equiv.), the yield of the product **3a** was reduced from 86% to 17%, and 1,1-diphenylethylene free radical adduct was isolated in 75% yield, which proved that the reaction proceeds through a radical pathway (Scheme 5a). Because of the open reaction system, the effect of O_2 in air on the reaction system was verified. When the model reaction was conducted under N_2, trace products were obtained. However, under an O_2 atmosphere, the yield of the product **3a** did not increase significantly, indicating that oxygen is a necessary component (Scheme 5b). Next, when the photosensitizer without the metal part was added to the model system, the reaction was completely

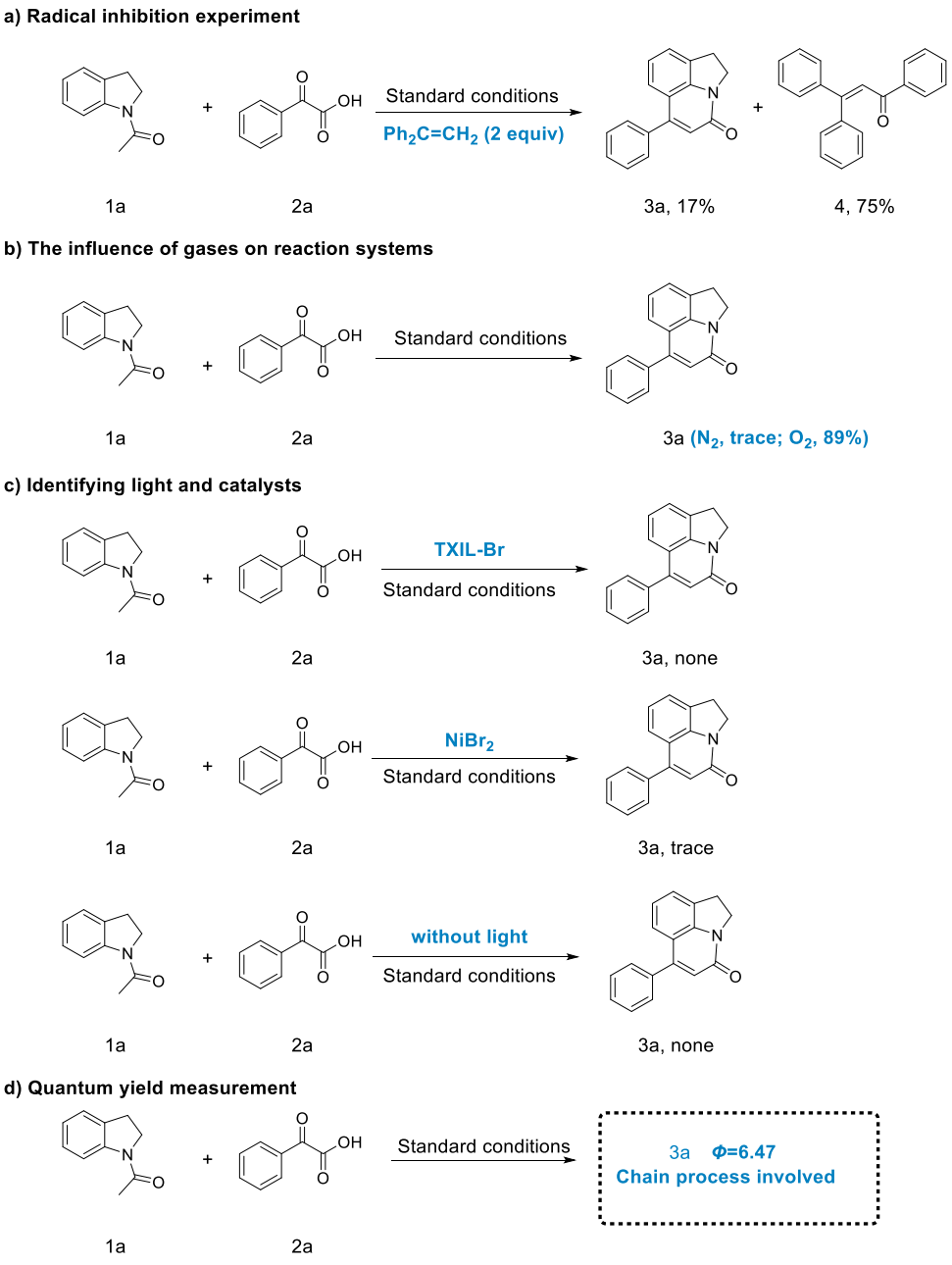

Scheme 5. Control experiments.

shut down, and the product **3a** was not observed. When only the metal catalyst $NiBr_2$ was added to the reaction system, the desired product **3a** was also not detected. This proved that photosensitizers and metal catalysts are essential for this reaction. Meanwhile, to investigate the interference of light on our strategy, the reaction under dark conditions proceeded. The experimental results indicated that light plays a necessary role in the reaction system (Scheme 5c). Finally, the measurement of quantum yield ($\Phi = 6.47 > 1$) of the model reaction under blue light irradiation, which suggests a radical-chain process might be involved in the reaction system [53] (see the **SI** for further details) (Scheme 5d).

Based on the above mechanism experiments and literature reports [54–58], a reasonable reaction mechanism was proposed, as shown in Fig. 4. Firstly, **TXIL-Ni**(II) is excited to form an excited state **TXIL-Ni**(II)* under visible light irradiation. The interaction between **TXIL-Ni**(II)* and the substrate **2a** generates benzoyl radical **A** and **TXIL-Ni**$(II)^{\bullet-}$ through a single election oxidation reaction, which is based on electrochemical and spectroscopic data (Fig. S11 in the **SI**). Next, the active nickel catalyst reacts with the substrate **1a** by chelation-directed C–H activation to form nickel cycle intermediate **B**, which undergoes oxidative addition with the formed benzoyl radical **A** *in situ* to afford a Ni(III) complex **C**. Subsequently, a ketone intermediate **D** and **TXIL-Ni**(I) are formed by the reductive elimination. Then, formed **TXIL-Ni**$(II)^{\bullet-}$ is further oxidized by O_2 in the air to regenerate **TXIL-Ni**(II) and produce superoxide radical ($O_2^{\bullet-}$), which was identified by electron paramagnetic resonance (EPR) to prove the existence of $O_2^{\bullet-}$ in the catalytic process [59–65] (Fig. 5). Density functional theory (DFT) calculations also further verified that the $O_2^{\bullet-}$ radical is generated in the catalytic cycle and the production of $O_2^{\bullet-}$ is a thermodynamically favorable process (for calculation details to see the **SI**, as shown in Fig. S13). The formed **TXIL-Ni**(I) is oxidized by $O_2^{\bullet-}$ to regenerate **TXIL-Ni**(II) and complete the catalytic cycle. Finally, in the presence of K_2CO_3, the target compound **3a** is obtained by Claisen-Schmidt condensation.

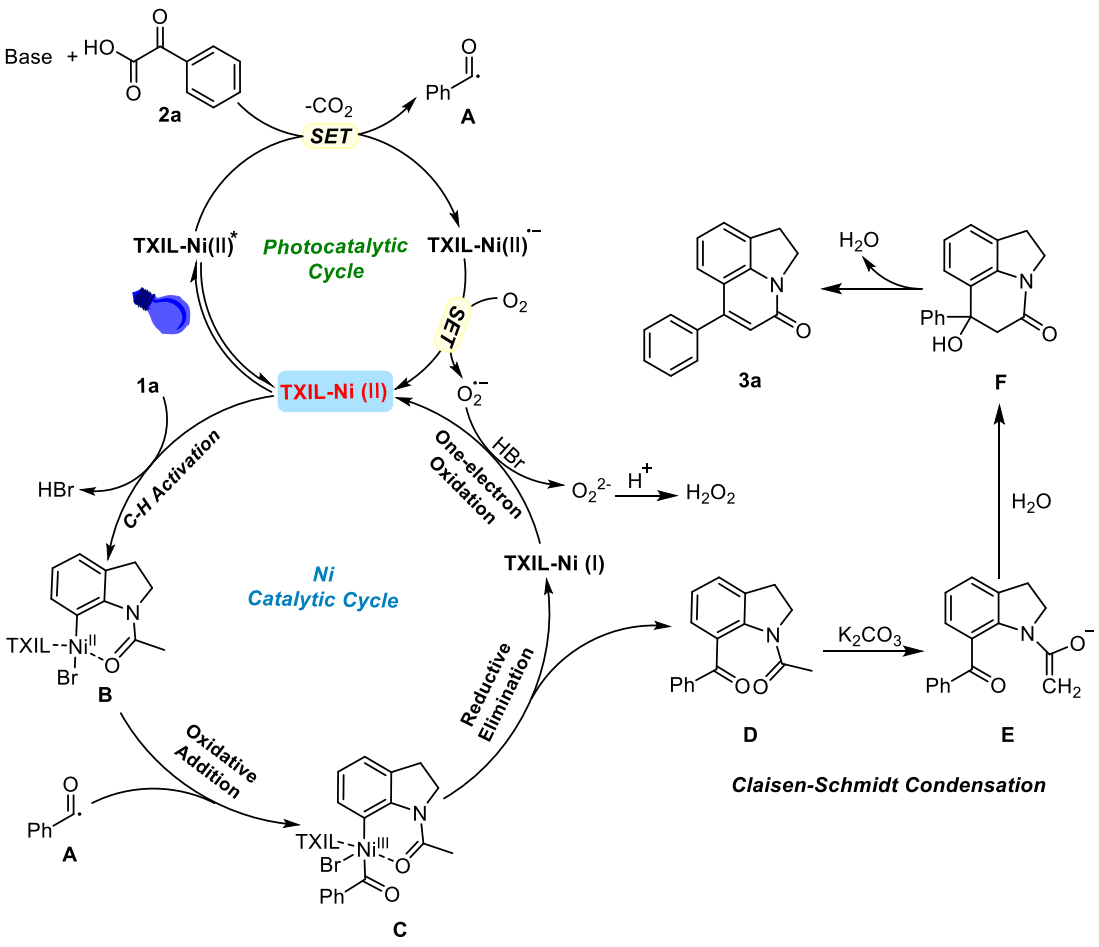

Fig. 4. Possible mechanism of the reaction.

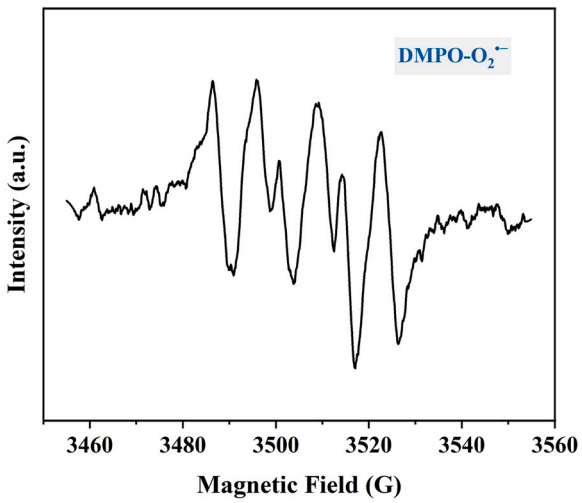

Fig. 5. EPR spectrum of a reaction mixture (**1a, 2a, TXIL-Ni**, K_2CO_3 and MeCN) and radical trap DMPO (0.1 M) under the irradiation of a blue LED.

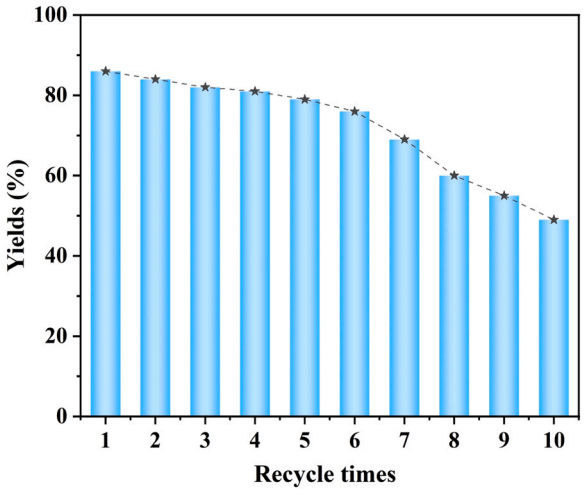

Fig. 6. Recyclability of **TXIL-Ni**.

3.5. Recyclability and comparison of catalytic performance

The reusability of catalysts is an important manifestation of green chemistry and sustainable development. Firstly, we conducted repeatability experiments on the use of new ionic liquid catalysts in model reactions. After completing the catalytic reaction, a small amount of water was added to the system for dilution, and the product was extracted into the organic phase using ethyl acetate as the extractant. The **TXIL-Ni** ionic liquid in the aqueous phase was directly used as the photocatalyst for the next reaction after the vacuum removal of water. The study showed that the catalyst could be recovered and reused six times with no obvious decrease in catalytic activity (Fig. 6). However, after increasing the reaction cycle, the yield of **3a** began to gradually decrease. This phenomenon was attributed to the structural composition of **TXIL-Ni** itself. This may be due to the volume difference between

Table 2
Comparison of catalytic and cycling performance of catalysts with other works.

Entry	Catalyst	Reaction Conditions	Yield (%)	Cyclic performance	Refs.
1	$[RhCp^*Cl_2]_2$	DCE, 100–120℃, 24 h	73%	None	[19]
2	$[\{RuCl_2(p\text{-cymene})\}_2]$	Tert-amyl alcohol, 130℃ 24 h	79%	None	[20]
3	$Cp^*Co(CO)I_2$	TFE, Ar, 110℃, 24 h	92%	None	[21]
4	$[Cp^*RhCl_2]_2$	MeOH, 80℃, 24 h	60%	None	[22]
5	$Cp^*Co(CO)I_2$	DCE, 120℃, 24 h	82%	None	[23]
6	NHC	THF, rt, 12 h	81%	None	[68]
7	**Our work**	**MeCN: H_2O, Air, rt, 24 h**	**86%**	**≥6 Runs**	**Here**

Abbreviations: DCE, 1,2-dichloroethane; TFE, 2,2,2-trifluoroethanol.

anions and cations, and the asymmetry of the structure. As the number of cycles increases, metal leaching led to a decrease in catalytic activity [66]. The Ni content in the recovered catalyst after 7 runs was determined to be 7.89 wt% via ICP-MS, which decreased compared to fresh catalysts (the Ni content in fresh catalyst was 8.83 wt%). Next, the TGA profile clearly indicated that **TXIL-Ni** catalyst is thermally stable up to 315 ℃ (Fig. S9 in the **SI**), which is beneficial for the reusability [67]. Finally, in order to further confirm the advantages of using new ionic liquid catalysts for the first time in the synthesis of pyrroloquinolinones, the catalytic and cyclic properties of **TXIL-Ni** were compared with the reported works (Table 2). In the different reports, the synthesis of pyrroloquinolinones was carried out at higher temperatures and the use of organic solvents, even toxic organic solvents. Therefore, the mild and green reaction conditions showed that the catalytic performance of the **TXIL-Ni** was highly competitive with the reported other works for the synthesis of pyrroloquinolinones so far. Cycle performance also had significant advantages compared to the reported transition-metal catalysts and organic catalysts currently [19–23,68].

4. Conclusions

In summary, **TXIL-Ni** as a novel bifunctional ionic liquid catalyst containing thioxanthone photosensitizer and transition metal Ni was designed and synthesized. The optical and electrical performance tests demonstrated that **TXIL-Ni** can serve as a photocatalyst due to its excellent photochemical properties and easy photoexcitation properties. **TXIL-Ni** successfully constructed pyrroloquinolinone derivatives through the tandem cyclization reaction of decarboxylation acylation and Claisen-Schmidt condensation under visible light irradiation. In addition, this method was used to synthesize the natural product Viridicatol and the intermediate of farnesyltransferase inhibitor. **TXIL-Ni** as a photocatalyst has the advantages of mild reaction conditions, green efficiency, and recyclability. The design and application of the new ionic liquid catalysts are still ongoing in our laboratory.

CRediT authorship contribution statement

Huixin Tong: Conceptualization, Data curation, Investigation, Methodology, Software, Writing – original draft preparation. **Mengqi Zou:** Supervision, Methodology, Investigation, Software. **Yuli Sha:** Formal analysis, Supervision. **Weiya Zhang:** Methodology, Investigation. **Houhai Fan:** Investigation. **Zhizhong Sun:** Resources, Supervision. **Wenyi Chu:** Resources, Supervision, Validation, Writing – review & editing, Project Administration, Funding Acquisition.

Declaration of Competing Interest

The authors declare that they have no known competing financial interests or personal relationships that could have appeared to influence the work reported in this paper.

Data Availability

Data will be made available on request.

Acknowledgements

This work was supported by the Project Supported by the Foundation for Engineering Technology Talent Training from Ministry of Education of China (Grant No. 19JDGC005); the Research Project of the Natural Science Foundation of Heilongjiang Province of China (LH2022B017).

Appendix A. Supporting information

Supplementary data associated with this article can be found in the online version at doi:10.1016/j.apcatb.2024.123835.

References

[1] S. Lucas, M. Negri, R. Heim, C. Zimmer, R.W. Hartmann, Fine-tuning the selectivity of aldosterone synthase inhibitors: structure−activity and structure−selectivity insights from studies of heteroaryl substituted 1,2,5,6-tetrahydropyrrolo[3,2,1-*ij*] quinolin-4-one derivatives, J. Med. Chem. 54 (2011) 2307–2319, https://doi.org/10.1021/jm101470k.
[2] E.A. Steak, L.T. Fletcher, C.D. Carabateas, Some 5,6-dihydro-4h-pyrrolo- [3,2,1-*i,j*] quinolines, J. Heterocycl. Chem. 11 (1974) 387–393, https://doi.org/10.1002/jhet.5570110321.
[3] D. Paris, M. Cottin, P. Demonchaux, G. Augert, P. Dupassieux, P. Lenoir, M.J. Peck, D. Jasserand, Synthesis, structure-activity relationships, and pharmacological evaluation of pyrrolo[3,2,1-*ij*]quinoline derivatives: Potent histamine and platelet activating factor antagonism and 5-lipoxygenase inhibitory properties. Potential therapeutic application in asthma, J. Med. Chem. 38 (1995) 669–685, https://doi.org/10.1021/jm00004a013.
[4] M. Isaac, A. Slassi, A. O'Brien, L. Edwards, N. MacLean, D. Bueschkens, D.K. Lee, K. McCallum, I. De Lannoy, L. Demchyshyn, R. Kamboj, Pyrrolo[3,2,1-*ij*]quinoline derivatives, a 5-HT_{2c} receptor agonist with selectivity over the 5-HT_{2a} receptor: potential therapeutic applications for epilepsy and obesity, Bioorg. Med. Chem. Lett. 10 (2000) 919–921, https://doi.org/10.1016/s0960-894x(00)00141-4.
[5] J.L. Stanton, M.H. Ackerman, Synthesis and anticonvulsant activity of some tetracyclic indole derivatives, J. Med. Chem. 26 (1983) 986–989, https://doi.org/10.1021/jm00361a010.
[6] L.N. Yin, Q.Z. Hu, R.W. Hartmann, Tetrahydropyrroloquinolinone type dual inhibitors of aromatase/aldosterone synthase as a novel strategy for breast cancer patients with elevated cardiovascular risks, J. Med. Chem. 56 (2013) 460–470, https://doi.org/10.1021/jm301408t.
[7] S.L. Ding, Y. Ji, Y. Su, R. Li, P.M. Gu, Schmidt reaction of ω-azido valeryl chlorides followed by intermolecular trapping of the rearrangement ions: synthesis of assoanine and related pyrrolophenanthridine alkaloids, J. Org. Chem. 84 (2019) 2012–2021, https://doi.org/10.1021/acs.joc.8b03018.
[8] Y.S. Yao, Q.X. Zhou, X.S. Wang, Y. Wang, B.W. Zhang, A DCM-type red-fluorescent dopant for high-performance organic electroluminescent devices, Adv. Funct. Mater. 17 (2007) 93–100, https://doi.org/10.1002/adfm.200600055.
[9] G. Antonio, C.R. Scholz, Methods of treating cancer patients with farnesyltransferase inhibitors, US20230089412A1[P], 2023-05-23.
[10] A. Safavi, E.S. Ghodousi, M. Ghavamizadeh, M. Sabaghan, O. Azadbakht, A. Veisi, H. Babaei, Z. Nazeri, M.K. Darabi, V. Zarezade, Computational investigation of novel farnesyltransferase inhibitors using 3D-QSAR pharmacophore modeling, virtual screening, molecular docking and molecular dynamics simulation studies: A new insight into cancer treatment, J. Mol. Struct. 1241 (2021) 130667, https://doi.org/10.1016/j.molstruc.2021.130667.
[11] K.H. Lee, M. Koh, A. Moon, Farnesyl transferase inhibitor FTI-277 inhibits breast cell invasion and migration by blocking H-Ras activation, Oncol. Lett. 12 (2016) 2222–2226, https://doi.org/10.3892/ol.2016.4837.
[12] A.L. Ho, I. Brana, R. Haddad, J. Bauman, K. Bible, S. Oosting, D.J. Wong, M.J. Ahn, V. Boni, C. Even, J. Fayette, M.J. Flor, K. Harrington, D.S. Hong, S.B. Kim, L. Licitra, I. Nixon, N.F. Saba, S. Hackenberg, P. Specenier, F. Worden, B. Balsara, M. Leoni, B. Martell, C. Scholz, A. Gualberto, Tipifarnib in head and neck squamous cell carcinoma with HRAS mutations, J. Clin. Oncol. 39 (2021) 1856–1864, https://doi.org/10.1200/JCO.20.02903.
[13] X.M. Ji, S.J. Zhou, C.L. Deng, F. Chen, R.Y. Tang, NH_4PF_6-promoted cyclodehydration of α-amino carbonyl compounds: efficient synthesis of pyrrolo [3,2,1-*ij*]quinoline and indole derivatives, RSC Adv. 4 (2014) 53837–53841, https://doi.org/10.1039/c4ra11168k.

[14] A. Padwa, P. Rashatasakhon, A.D. Ozdemir, J. Willis, A study of vinyl radical cyclization using N-alkenyl-7-bromo-substituted hexahydroindolinones, J. Org. Chem. 70 (2005) 519–528, https://doi.org/10.1021/jo048314i.
[15] M. Layek, A.V.D. Rao, V. Gajare, D. Kalita, D.K. Barange, A. Islam, K. Mukkanti, M. Pal, C−N bond forming reaction under copper catalysis: a new synthesis of 2-substituted 5,6-dihydro-4*H*-pyrrolo[3,2,1-*ij*]-quinolines, Tetrahedron Lett. 50 (2009) 4878–4881, https://doi.org/10.1016/j.tetlet.2009.06.041.
[16] A. Tsotinis, M. Panoussopoulou, A. Eleutheriades, K. Davidson, D. Sugden, Design, synthesis and melatoninergic activity of new unsubstituted and β,β′-difunctionalised 2,3-dihydro-1*H*-pyrrolo[3,2,1-*ij*]quinolin-6-alkanamides, Eur. J. Med. Chem. 42 (2007) 1004–1013, https://doi.org/10.1016/j.ejmech.2007.01.005.
[17] S. Rajput, C.W. Leu, K. Wood, D.S.C. Black, N. Kumar, Facile syntheses of 7,9-dimethoxypyrrolo[3,2,1-*ij*]-quinolin-6-ones, Tetrahedron Lett. 52 (2011) 7095–7098, https://doi.org/10.1016/j.tetlet.2011.10.089.
[18] J.H. Docherty, T.M. Lister, G. McArthur, M.T. Findlay, P. Domingo-Legarda, J. Kenyon, S. Choudhary, I. Larrosa, Transition-metal-catalyzed C-H bond activation for the formation of C-C bonds in complex molecules, Chem. Rev. 123 (2023) 7692–7760, https://doi.org/10.1021/acs.chemrev.2c00888.
[19] X.F. Yang, X.H. Hu, T.P. Loh, Expedient synthesis of pyrroloquinolinones by Rh-catalyzed annulation of N-carbamoyl indolines with alkynes through a directed C−H functionalization/C−N cleavage sequence, Org. Lett. 17 (2015) 1481–1484, https://doi.org/10.1021/acs.orglett.5b00355.
[20] R. Manoharan, M. Jeganmohan, Ruthenium-catalyzed cyclization of N-carbamoyl indolines with alkynes: an efficient route to pyrroloquinolinones, Org. Biomol. Chem. 13 (2015) 9276–9284, https://doi.org/10.1039/c5ob01146a.
[21] R. Mandal, B. Garai, B. Sundararaju, Cp^*Co^{III}-catalyzed C(7)–H bond annulation of indolines with alkynes, J. Org. Chem. 86 (2021) 9407–9417, https://doi.org/10.1021/acs.joc.1c00713.
[22] X. Wang, H.Y. Tang, H.J. Feng, Y.C. Li, Y.X. Yang, B. Zhou, Access to six- and seven-membered 1,7-fused indolines via Rh(III)-catalyzed redox-neutral C7-selective C-H functionalization of indolines with alkynes and alkenes, J. Org. Chem. 80 (2015) 6238–6249, https://doi.org/10.1021/acs.joc.5b00684.
[23] S.K. Banjare, P. Biswal, P.C. Ravikumar, Cobalt-catalyzed one-step access to pyroquilon and C-7 alkenylation of indoline with activated alkenes using weakly coordinating functional groups, J. Org. Chem. 85 (2020) 5330–5341, https://doi.org/10.1021/acs.joc.0c00023.
[24] N. Holmberg-Douglas, D.A. Nicewicz, Photoredox-catalyzed C-H functionalization reactions, Chem. Rev. 122 (2022) 1925–2016, https://doi.org/10.1021/acs.chemrev.1c00311.
[25] C.K. Prier, D.A. Rankic, D.W.C. MacMillan, Visible light photoredox catalysis with transition metal complexes: applications in organic synthesis, Chem. Rev. 113 (2013) 5322–5363, https://doi.org/10.1021/cr300503r.
[26] C.L. Wang, J.Y. Qao, X.C. Liu, H. Song, Z.Z. Sun, W.Y. Chu, Visible-light-induced decarboxylation coupling/intramolecular cyclization: a one-pot synthesis for 4-aryl-2-quinolinone derivatives, J. Org. Chem. 83 (2018) 1422–1430, https://doi.org/10.1021/acs.joc.7b02979.
[27] Q. Shi, P.H. Li, X.J. Zhu, L. Wang, Decarboxylative/decarbonylative C3-acylation of indoles via photocatalysis: a simple and efficient route to 3-acylindoles, Green. Chem. 18 (2016) 4916–4923, https://doi.org/10.1039/c6gc00516k.
[28] H.L. Zhu, F.L. Zeng, X.L. Chen, K. Sun, H.C. Li, X.Y. Yuan, L.B. Qu, B. Yu, Acyl radicals from α-keto acids: Metal-free visible-light-promoted acylation of heterocycles, Org. Lett. 23 (2021) 2976–2980, https://doi.org/10.1021/acs.orglett.1c00655.
[29] G.L. Xie, Y.H. Zhao, C.Q. Cai, G.J. Deng, H. Gong, Palladium-catalyzed direct and specific C-7 acylation of indolines with 1,2-diketones, Org. Lett. 23 (2021) 410–415, https://doi.org/10.1021/acs.orglett.0c03922.
[30] K.P.S. Cheung, S. Sarkar, V. Gevorgyan, Visible light-induced transition metal catalysis, Chem. Rev. 122 (2022) 1543–1625, https://doi.org/10.1021/acs.chemrev.1c00403.
[31] N.A. Romero, D.A. Nicewicz, Organic photoredox catalysis, Chem. Rev. 116 (2016) 10075–10166, https://doi.org/10.1021/acs.chemrev.6b00057.
[32] B.K. Kundu, C. Han, P. Srivastava, S. Nagar, K.E. White, J.A. Krause, C.G. Elles, Y. J. Sun, Trifluoromethylative bifunctionalization of alkenes via a bibenzothiazole-derived photocatalyst under both visible- and near-infrared-light irradiation, ACS Catal. 13 (2023) 8119–8127, https://doi.org/10.1021/acscatal.3c01812.
[33] A.B. Rolka, B. Koenig, Dearomative cycloadditions utilizing an organic photosensitizer: an alternative to iridium catalysis, Org. Lett. 22 (2020) 5035–5040, https://doi.org/10.1021/acs.orglett.0c01622.
[34] L.D. Elliott, S. Kayal, M.W. George, K. Booker-Milburn, Rational design of triplet sensitizers for the transfer of excited state photochemistry from uv to visible, J. Am. Chem. Soc. 142 (2020) 14947–14956, https://doi.org/10.1021/jacs.0c05069.
[35] W.J. Kang, B. Li, M. Duan, G.X. Pan, W.Q. Sun, A.S. Ding, Y.B. Zhang, K.N. Houk, H. Guo, Discovery of a thioxanthone-TfOH complex as a photoredox catalyst for hydrogenation of alkenes using *p*-xylene as both electron and hydrogen sources, Angew. Chem. Int. Ed. 61 (2022) e202211562, https://doi.org/10.1002/anie.202211562.
[36] P. Wasserscheid, W. Keim, Ionic liquids-new "solutions" for transition metal catalysis, Angew. Chem. Int. Ed. 39 (2000) 3772–3789, https://doi.org/10.1002/1521-3773(20001103)39:21<3772::AIDANIE3772>3.0.CO;2-5.
[37] F. Shirzaei, H.R. Shaterian, Preparation of novel functionalized ionic liquid: green, stable, and reusable catalyst for the synthesis of new 2-(phenylsulfonyl)-1*H*-benzo [a]pyrano[2,3-c]phenazin-3-amine derivatives, J. Mol. Liq. 345 (2022) 117893, https://doi.org/10.1016/j.molliq.2021.117893.
[38] J.P. Hallett, T. Welton, Room-temperature ionic liquids: solvents for synthesis and catalysis. 2, Chem. Rev. 111 (2011) 3508–3576, https://doi.org/10.1021/cr1003248.
[39] P. Migowski, P. Lozano, J. Dupont, Imidazolium based ionic liquid-phase green catalytic reactions, Green. Chem. 25 (2023) 1237–1260, https://doi.org/10.1039/d2gc04749g.
[40] S. Rengshausen, C. Van Stappen, N. Levin, S. Tricard, K.L. Luska, S. DeBeer, B. Chaudret, A. Bordet, W. Leitner, Organometallic synthesis of bimetallic cobalt-rhodium nanoparticles in supported ionic liquid phases (coxrh100-x@silp) as catalysts for the selective hydrogenation of multifunctional aromatic substrates, Small 17 (2021) 2006683, https://doi.org/10.1002/smll.202006683.
[41] N.V. Plechkova, K.R. Seddon, Applications of ionic liquids in the chemical industry, Chem. Soc. Rev. 37 (2008) 123–150, https://doi.org/10.1039/b006677j.
[42] Y.L. Gu, G.X. Li, Ionic liquids-based catalysis with solids: state of the art, Adv. Synth. Catal. 351 (2009) 817–847, https://doi.org/10.1002/adsc.200900043.
[43] K. Li, H. Choudhary, R.D. Rogers, Ionic liquids for sustainable processes: liquid metal catalysis, Curr. Opin. Green. Sustain. Chem. 11 (2018) 15–21, https://doi.org/10.1016/j.cogsc.2018.02.011.
[44] X.H. Zhu, W.P. Li, H. Yan, R.G. Zhong, Triplet phenacylimidazoliums-catalyzed photocycloaddition of 1,4-dihydropyridines: an experimental and theoretical study, J. Photochem. Photobiol. A-Chem. 241 (2012) 13–20, https://doi.org/10.1016/j.jphotochem.2012.05.013.
[45] M.G. Ahmad, K. Chanda, Ionic liquid coordinated metal-catalyzed organic transformations: a comprehensive review, Coord. Chem. Rev. 472 (2022) 214769, https://doi.org/10.1016/j.ccr.2022.214769.
[46] N. Azizi, F. Shirdel, Task specific dicationic acidic ionic liquids catalyzed efficient and rapid synthesis of benzoxanthenones derivatives, J. Mol. Liq. 222 (2016) 783–787, https://doi.org/10.1016/j.molliq.2016.07.128.
[47] H.F. Ni, Y.W. Zhang, C.H. Zong, Z.B. Hou, H. Song, Y. Chen, X.S. Liu, T.F. Xu, Y. J. Luo, Synthesis of tropine-based functionalized acidic ionic liquids and catalysis of esterification, Int. J. Mol. Sci. 23 (2022) 12877, https://doi.org/10.3390/ijms232112877.
[48] P. Liang, Y.Y. Zhang, P. Yang, S. Grond, Y. Zhang, Z.-J. Qian, Viridicatol and viridicatin isolated from a shark-gill-derived fungus penicilliumpolonicum AP2T1 as MMP-2 and MMP-9 inhibitors in HT1080 cells by mapks signaling pathway and docking studies, Med. Chem. Res. 28 (2019) 1039–1048, https://doi.org/10.1007/s00044-019-02358-w.
[49] P.R. Angibaud, M.G. Venet, W. Filliers, R. Broeckx, Y.A. Ligny, P. Muller, V. S. Poncelet, D.W. End, Synthesis routes towards the farnesyl protein transferase inhibitor ZARNESTRA™, Eur. J. Org. Chem. 2004 (2004) 479–486, https://doi.org/10.1002/ejoc.200300538.
[50] P.R. Angibaud, M.G. Venet, 1,8-annelated quinoline derivatives substituted with carbon-linked triazoles as farnesyl transferase inhibitors, US07408063B2[P], 2008-08-05.
[51] P. Angibaud, X. Bourdrez, A. Devine, D.W. End, E. Freyne, Y. Ligny, P. Muller, G. Mannens, I. Pilatte, V. Poncelet, S. Skrzat, G. Smets, J. Van Dun, P. Van Remoortere, M. Venet, W. Wouters, 5-imidazolyl-quinolinones, -quinazolinones and -benzo-azepinones as farnesyltransferase inhibitors, Bioorg. Med. Chem. Lett. 13 (2003) 1543–1547, https://doi.org/10.1016/S0960-894X(03)00180-X.
[52] V.A. Mamedoy, V.L. Mamedova, S.F. Kadyrova, V.R. Galimullina, G.Z. Khikmatoya, D.E. Korshin, A.T. Gubaidullin, D.B. Krivolapov, I.K. Rizyanov, O.B. Bazanova, O. G. Sinyashin, S.K. Latypov, Synthesis of 3-hydroxy-4-arylquinolin-2-ones including viridicatol via a darzens condensation/friedel-crafts alkylation strategy, J. Org. Chem. 83 (2018) 13132–13145, https://doi.org/10.1021/acs.joc.8b01871.
[53] K.J. Liang, N. Li, Y. Zhang, T. Li, C.F. Xia, Transition-metal-free α-arylation of oxindoles via visible-light-promoted electron transfer, Chem. Sci. 10 (2019) 3049–3053, https://doi.org/10.1039/c8sc05170d.
[54] S.Y. Yan, Y.J. Liu, B. Liu, Y.H. Liu, B.F. Shi, Nickel-catalyzed thiolation of unactivated aryl C-H bonds: efficient access to diverse aryl sulfides, Chem. Commun. 51 (2015) 4069–4072, https://doi.org/10.1039/c4cc10446c.
[55] J. Xu, L. Qiao, J.B. Shen, K.J. Chai, C. Shen, P.F. Zhang, Nickel(II)-catalyzed site-selective C-H bond trifluoromethylation of arylamine in water through a coordinating activation strategy, Org. Lett. 19 (2017) 5661–5664, https://doi.org/10.1021/acs.orglett.7b02823.
[56] G.S. Lee, J. Won, S. Choi, M.H. Baik, S.H. Hong, Synergistic activation of amides and hydrocarbons for direct C(sp3)–H acylation enabled by metallaphotoredox catalysis, Angew. Chem. Int. Ed. 59 (2020) 16933–16942, https://doi.org/10.1002/anie.202004441.
[57] C. Zhou, P.H. Li, X.J. Zhu, L. Wang, Merging photoredox with palladium catalysis: decarboxylative *ortho*-acylation of acetanilides with α-oxocarboxylic acids under mild reaction conditions, Org. Lett. 17 (2015) 6198–6201, https://doi.org/10.1021/acs.orglett.5b03192.
[58] D.L. Zhu, Q. Wu, D.J. Young, H. Wang, Z.G. Ren, H.X. Li, Acyl radicals from α-keto acids using a carbonyl photocatalyst: photoredox-catalyzed synthesis of ketones, Org. Lett. 22 (2020) 6832–6837, https://doi.org/10.1021/acs.orglett.0c02351.
[59] X.W. Gao, Q.Y. Meng, M. Xiang, B. Chen, K. Feng, C.H. Tung, L.Z. Wu, Combining visible light catalysis and transition metal catalysis for the alkylation of secondary amines, Adv. Synth. Catal. 355 (2013) 2158–2164, https://doi.org/10.1002/adsc.201300311.
[60] J.J. Zhong, Q.Y. Meng, G.X. Wang, Q. Liu, B. Chen, K. Feng, C.H. Tung, L.Z. Wu, A highly efficient and selective aerobic cross-dehydrogenative-coupling reaction photocatalyzed by a platinum(II) terpyridyl complex, Chem. -Eur. J. 19 (2013) 6443–6450, https://doi.org/10.1002/chem.201204572.
[61] D.C. Fabry, J. Zoller, S. Raja, M. Rueping, Combining rhodium and photoredox catalysis for C-H functionalizations of arenes: oxidative heck reactions with visible

light, Angew. Chem. Int. Ed. 53 (2014) 10228–10231, https://doi.org/10.1002/anie.201400560.
[62] J. Liu, Q. Liu, H. Yi, C. Qin, R.P. Bai, X.T. Qi, Y. Lan, A.W. Lei, Visible-light-mediated decarboxylation/oxidative amidation of α-keto acids with amines under mild reaction conditions using O_2, Angew. Chem. Int. Ed. 53 (2014) 502–506, https://doi.org/10.1002/anie.201308614.
[63] D.C. Fabry, M.A. Ronge, J. Zoller, M. Rueping, C-H functionalization of phenols using combined ruthenium and photoredox catalysis: in situ generation of the oxidant, Angew. Chem. Int. Ed. 54 (2015) 2801–2805, https://doi.org/10.1002/IIanie.201408891.
[64] J. Zoller, D.C. Fabry, M.A. Ronge, M. Rueping, Synthesis of indoles using visible light: photoredox catalysis for palladium-catalyzed C-H activation, Angew. Chem., Int. Ed. 53 (2014) 13264–13268, https://doi.org/10.1002/anie.201405478.
[65] Q. Shi, P.H. Li, X.J. Zhu, L. Wang, Decarboxylative/decarbonylative C3-acylation of indoles *via* photocatalysis: a simple and efficient route to 3-acylindoles, Green. Chem. 18 (2016) 4916–4923, https://doi.org/10.1039/c6gc00516k.
[66] M. Varyani, P.K. Khatri, S.L. Jain, Amino acid ionic liquid bound copper schiff base catalyzed highly efficient three component A^3-coupling reaction, Catal. Commun. 77 (2016) 113–117, https://doi.org/10.1016/j.catcom.2016.01.020.
[67] N. Yao, M. Lu, X.B. Liu, J. Tan, Y.L. Hu, Copper-doped mesoporous silica supported dual acidic ionic liquid as an efficient and cooperative reusability catalyst for biginelli reaction, J. Mol. Liq. 262 (2018) 328–335, https://doi.org/10.1016/j.molliq.2018.04.121.
[68] X.Y. Duan, Z.H. Tian, B.H. Liu, T. He, L.L. Zhao, M.D. Dong, P.N. Zhang, J. Qi, Highly enantioselective synthesis of pyrroloindolones and pyrroloquinolinones via an N-heterocyclic carbene-catalyzed cascade reaction, Org. Lett. 23 (2021) 3777–3781, https://doi.org/10.1021/acs.orglett.1c01203.